

Anoxia-Induced Changes in Pyridine Nucleotide Redox State in Cortical Neurons and Astrocytes

Sibel Kahraman · Gary Fiskum

Accepted: 16 October 2006 / Published online: 27 December 2006
© Springer Science+Business Media, LLC 2006

Abstract NAD(P)H autofluorescence was used to verify establishment of metabolic anoxia using primary cultures of cortical neurons and astrocytes. Cells on cover slips were placed in a chamber and O₂ was displaced by continuous infusion of argon. Perfusion with medium at PO₂ < 0.4 mm Hg caused an increase in NAD(P)H fluorescence, albeit to levels lower than that obtained with cyanide. Addition of the nitric oxide-generating agent DETA-NO to the hypoxic medium further increased fluorescence to the level with cyanide. Fluorescence under anoxia remained high in the presence of glucose, but declined in neurons and not in astrocytes when glucose was substituted with 2-deoxyglucose. Reoxygenation of neurons resulted in a decline in fluorescence and a loss in fluorescent gradient between fully reduced and fully oxidized (plus respiratory uncoupler). We conclude that (1) DETA-NO is useful for generating metabolic anoxia in the presence of argon (2) Exogenous glucose is necessary to maintain NAD(P)H in a reduced state during metabolic anoxia in neurons but not astrocytes (3) Neurons undergo a partially irreversible decline in NAD(P)H fluorescence during metabolic anoxia and reoxygenation that could contribute to prolonged metabolic failure.

Keywords Mitochondria · Cytochrome oxidase · Nitric oxide · Fluorescence · Respiration

Introduction

The intrinsic fluorescence of reduced nicotinamide adenine dinucleotide (NADH), the principal electron shuttle molecule in both the cytosolic and mitochondrial compartments, is a sensitive indicator of changes in energy metabolism and of oxidative stress [1–3]. While the fluorescence profile of reduced nicotinamide adenine dinucleotide phosphate (NADPH) is indistinguishable from that of NADH [4], the contribution of NADPH to the intrinsic fluorescence of cellular reduced pyridine nucleotides is small, relative to that of NADH [5–6].

During ischemic insults, both oxidative and glycolytic metabolism are impaired following depletion of O₂ and glucose, leading to a reduced shift in the redox state of NADH [7]. Studies performed both *in vivo* and *in vitro* suggest that reperfusion after ischemia or reoxygenation after hypoxia leads to NAD(P)H hyperoxidation [8–10]. Studies describing NAD(P)H autofluorescence changes throughout ischemia/reperfusion in brain tissue or slices do not reveal the respective contribution of neurons and glial cells to the global emission. However, characterization of distinctive changes in NADH signal in neurons and astrocytes, as defined by Kasischke et al [11] in hippocampal slices during focal neural activity, is essential to provide better understanding of interactions between glial and neuronal compartment during cerebral ischemia. Moreover, hypoxia studies with cultured neurons and astrocytes are typically performed under levels of

Special issue dedicated to John P. Blass.

S. Kahraman · G. Fiskum
Anesthesiology, Program in Neuroscience, University of
Maryland School of Medicine, Baltimore, MD 21201, USA

S. Kahraman · G. Fiskum (✉)
Anesthesiology Research Labs., University of Maryland
School of Medicine, 685 W Baltimore Street, MSTF 5-34,
Baltimore, MD 21201, USA
e-mail: gfishk001@umaryland.edu

O₂ that do not simulate *in vivo* ischemic conditions and therefore may not represent metabolic anoxia, where respiration ceases due to insufficient O₂ as substrate for the cytochrome oxidase reaction of the electron transport chain.

In this study, we established a fluorescence microscopy perfusion system that induces true metabolic anoxia in cell cultures and examined the changes in cellular NAD(P)H redox state to provide a better understanding of metabolic regulation during anoxia/reoxygenation in cortical neurons and astrocytes.

Experimental procedure

Materials

All cell culture reagents were from GIBCO-BRL. Potassium cyanide (KCN) was purchased from Fisher Scientific Company L.L.C. (Pittsburgh, USA). Unless otherwise stated, all other chemicals were obtained from Sigma-Aldrich Inc. (St Louis, MO, USA).

Cell culture

Cortical neurons were isolated from 17th day *in utero* Sprague-Dawley rats. All animal procedures were carried out according to the National Institutes of Health and the University of Maryland, Baltimore guidelines for the care and use of laboratory animal. Cortical neurons were grown on 25 mm coverslips for 10–14 days *in vitro*, at a density of ~ 50,000 cells/coverslip, using DMEM, glutamine, neurobasal medium and B27 supplement in 95% air / 5% CO₂ at 37°C. Glial proliferation was prevented by adding cytosine-arabinoxanthine (5 μM) 24 h after plating. Immunocytochemical measurements of glial fibrillary acid protein (GFAP) confirmed that cultures contained <1% glia. Cortical astrocytes cultured in DMEM/F12 (1/1) 10% FBS with penicillin and streptomycin in 95% air / 5% CO₂ at 37°C at a density of ~ 200,000 cells/coverslip. The culture medium of cortical astrocyte culture was changed every 3 days and the cells were used at 14–17 div within 48 h after changing medium. Cultures were >95% astrocytes by GFAP immunocytochemistry.

Fluorescence microscopy

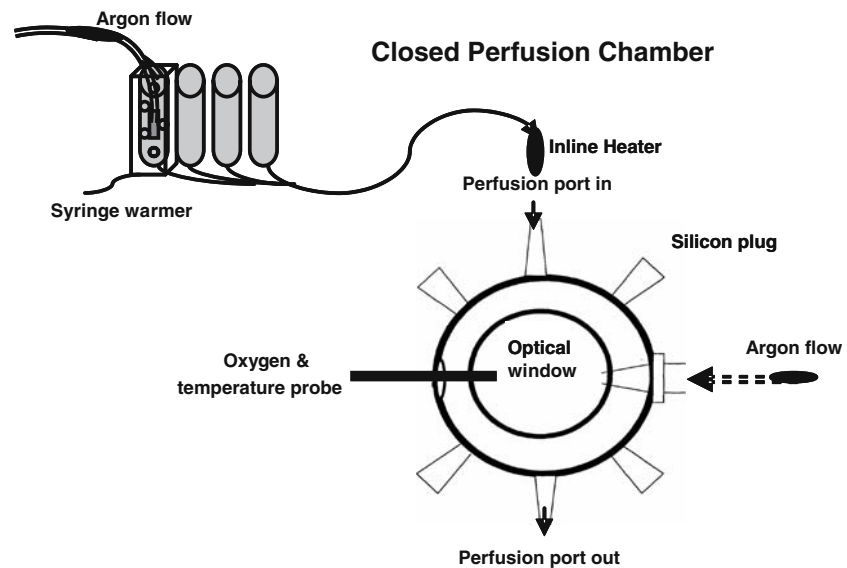
Primary cultures of rat cortical neurons and astrocytes on 25 mm glass coverslips were placed in the bottom of the closed perfusion micro-incubator (LU-CPC-CEH, Harvard Apparatus, Inc., Holliston, MA, USA). For all

experiments, the cells in the chamber were constantly perfused at 0.5 ml/min with pH 7.4 artificial cerebrospinal fluid (aCSF) containing 120 mM NaCl, 3.5 mM KCl, 1.3 mM CaCl₂, 0.4 mM KH₂PO₄, 1 mM MgCl₂, 20 mM HEPES, 15 mM glucose/2 mM 2-deoxyglucose. Syringe reservoirs were continuously bubbled with either air or ultra-high purity argon to displace O₂ from a cylinder through a line that perforates the gas impermeable caps (Qubit systems, Ontario, Canada) of syringe reservoirs (Fig. 1). The pressure inside the reservoir was released by a small opening on the reservoir cap. Tygon tubing that is less permeable to O₂ than the conventional tubing was used for the anoxic perfusion. Additionally, the tubing length from the perfusion syringe to the chamber was kept as short as possible. Argon was also infused directly in the chamber from one of the eight side-ports of the chamber to create a gas curtain over the perfusate, preventing re-entry of O₂ from the atmosphere to the argon-bubbled perfusate. Two of the ports served as either inlet or outlet for perfusion. Another port served as access for the O₂ and temperature probes. The rest of the ports were kept closed by using thick silicon plugs. The gas and perfusate were heated with a single and multi-line solution in-line heater, respectively (Harvard Apparatus, Inc., Holliston, MA, USA), and the solution reservoirs were heated by separate syringe warmers (Harvard Apparatus, Inc., Holliston, MA, USA). These together with the microscope chamber platform heater (TC-202A temperature controller, Harvard Apparatus, Inc., Holliston, MA, USA) were used in combination to provide efficient thermal regulation. The PO₂ and temperature of the perfusate in the chamber were monitored continuously by a fiber-optic microprobe (OxyLite, Oxford Optronix Ltd, Oxford, UK).

The closed perfusion chamber was mounted on a Nikon Eclipse TE2000-S inverted microscope (SFluor 20 × 0.75 N.A.). Single cell autofluorescence of NAD(P)H was imaged by excitation at 355 nm (Polychrome IV, Till, Munich, Germany), and emission above 420 nm wavelengths. Image sequences (10 s/frame, 120 ms exposure time, 4 × 4 binning) were acquired by an ORCA-ER cooled digital CCD camera (Hamamatsu Photonics, Hamamatsu, Germany) and imaged with Metafluor 6.3 (Universal Imaging, West Chester, PA) imaging software.

When added, diethylenetriamine/nitric oxide adduct (DETA-NO, Sigma-Aldrich, St Louis, MO, USA), at a final concentration of 50 μM, was present in the perfusate throughout the experiment. DETA-NO was added in aCSF 30 min before starting to perfuse the cells to achieve the stable concentrations of NO in the

Fig. 1 Microscopy perfusion system used to measure NAD(P)H epifluorescence during hypoxia and reoxygenation using cortical neurons and astrocytes cultured on coverslips



aCSF. 30 min of argon-flushed anoxic perfusion was followed by 10 min of reoxygenation. At the end of each anoxia experiment, cells were perfused with 1 mM of potassium cyanide (KCN, Fischer Chemical, USA), and 5 μ M of carbonyl cyanide *p*-trifluoromethoxyphenyl hydrazone (FCCP, Sigma-Aldrich, St Louis, MO, USA) to assess the maximum and minimum signal in individual cells when the electron transport chain was first completely inhibited and then completely uncoupled, respectively. The NAD(P)H autofluorescence was expressed as the normalized epifluorescence change ($\Delta f/f_0$), which is the difference in fluorescence ($\Delta f = f_1 - f_0$) normalized to the basal fluorescence (f_0).

Statistical analysis

All experiments were performed on three coverslips from three separate cultures of either cortical neurons or astrocytes. Statistical significance was assessed by one-way ANOVA test followed by the Tukey test for multiple comparisons. Data with a heterogeneous variance were assessed by Mann–Whitney *U*-test. All data are expressed as means \pm S.E.M. of *n* cells measured from three cover slips. The point of minimum acceptable statistical significance was taken to be 0.05.

Results

Establishment of metabolic anoxia in cell cultures

Superfusion of both cortical neurons and astrocytes for 60 min or more with aCSF resulted in no change in

NAD(P)H autofluorescence, indicating that image acquisitions obtained every 10 s caused no photobleaching or phototoxicity (Fig. 2). In addition, the presence of up to 200 μ M DETA-NO in the perfusate did not cause a change in baseline NAD(P)H autofluorescence either in cortical neuronal or astrocytic cultures.

When cells were exposed to argon infusion, PO_2 values of the perfusate present in the chamber fell to < 0.4 mm Hg within 5 min. In cortical neurons, this level of hypoxia resulted in a moderate increase in NAD(P)H autofluorescence that was not, however, as great as the maximum obtained in the presence of 1 mM KCN (0.263 ± 0.014 vs 0.375 ± 0.010 , $P < 0.001$) (Fig. 3A). Experiments were then performed to determine if the lack of complete pyridine nucleotide reduction with argon was due to the presence of residual O_2 at a concentration that is capable of sustaining at least some flow of electrons through mitochondrial respiration. Taking advantage of the competitive inhibition that occurs between nitric oxide and O_2 at cytochrome oxidase [12–13], we tested the ability of the nitric oxide-generating molecule DETA-NO to raise the level of NAD(P)H fluorescence in the presence of argon to the level obtained by cyanide. While DETA-NO did not cause any change in NAD(P)H fluorescence in normal, air-saturated media, the presence of 50 μ M DETA-NO in the argon-bubbled perfusate resulted in an increase of $\Delta f/f_0$ to 0.420 ± 0.019 (Fig. 3A). This degree of reduction was essentially equivalent to the rise in NAD(P)H autofluorescence obtained in the presence of 1 mM KCN. The combination of DETA-NO plus argon was therefore used to model the influence of metabolic anoxia

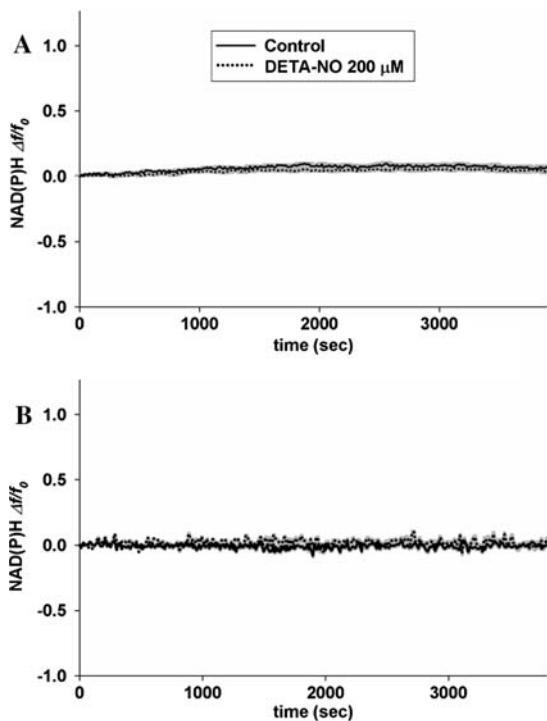


Fig. 2 NAD(P)H fluorescence measurements under normoxic conditions using primary cultures of cortical neurons (**A**) and cortical astrocytes (**B**) in the absence and presence of nitric oxide. Images acquired every 10 s with exposure time of 120 ms and 4×4 binning, for 1 h. Solid lines represent the mean of fluorescence in neuron somata in the field ($n = 30\text{--}50$) in control cultures, and dashed lines represent the mean fluorescence during perfusion with DETA-NO $200 \mu\text{M}$; gray shadows represent SEM

on pyridine nucleotide fluorescence in neurons and astrocytes.

NAD(P)H autofluorescence of cortical neurons and astrocytes during anoxia

Anoxic perfusion caused a rapid increase in NAD(P)H autofluorescence in both cortical neurons and astrocytes (0.420 ± 0.019 and 0.302 ± 0.017 , respectively), as demonstrated by the fluorescent images shown in Fig. 3. B,C. As expected, fluorescence abruptly declined to a level lower than the initial baseline following reoxygenation and the addition of the respiratory uncoupler FCCP.

In the presence of glucose, NAD(P)H autofluorescence remained high throughout anoxia in both cell types (Fig. 4). During cerebral ischemia, brain cells are deprived of exogenous glucose as well as O_2 . We therefore tested the effect of glucose deprivation in addition to metabolic anoxia on pyridine nucleotide fluorescence. While the initial rise in fluorescence elicited by perfusion with argon-saturated medium

containing DETA-NO in the absence of glucose and the presence of 2-deoxyglucose was similar to the changes observed in the presence of glucose for both cell types, the NAD(P)H fluorescence spontaneously and gradually declined in the glucose-deprived neurons but not astrocytes (Fig. 5). In fact, by the end of the period of anoxia, the fluorescence in neurons returned to approximately the baseline value.

NAD(P)H autofluorescence of cortical neurons and astrocytes during reoxygenation

During reperfusion with air-saturated medium containing glucose, following 30 min anoxia, pyridine nucleotide fluorescence declined past the pre-anoxia baseline value by -0.029 ± 0.002 ($p = 0.004$) in neurons but not in astrocytes (-0.020 ± 0.021 , $p = 0.150$), as also demonstrated in Fig. 6. When anoxic perfusion included the substitution of 2-deoxyglucose for glucose, reoxygenation resulted in a decline in fluorescence of -0.266 ± 0.068 ($p = 0.001$) compared to the original baseline fluorescence in neurons, whereas a much smaller decline of -0.041 ± 0.009 ($P = 0.001$) occurred in astrocytes (Fig. 6A). This reoxygenation-induced decay of baseline NAD(P)H autofluorescence occurred immediately after the start of reoxygenation with no apparent recovery over time.

The post-anoxic decline in pyridine nucleotide fluorescence could be due to net oxidized shift in redox state or due to other factors, e.g. a reduction in the total cellular pyridine nucleotide content. To differentiate between these possibilities, we approximated the total pyridine nucleotide fluorescence by calculating the fluorescence gradient between maximum fluorescence produced by KCN and minimum fluorescence produced by exposure to the respiratory uncoupler FCCP in cells after incubation at equivalent times using either normal medium or argon-bubbled medium plus DETA-NO in the absence or presence of glucose (+ 2-deoxyglucose) (Fig. 6B). The fluorescence gradient obtained for either neurons or astrocytes after exposure to metabolic anoxia plus glucose was no different than that obtained after incubation under normal, control conditions. When glucose was replaced with 2-deoxyglucose, the pyridine nucleotide fluorescence gradient was significantly, approximately 33% lower in neurons than that obtained after control incubations; however, this effect of glucose deprivation plus metabolic anoxia was not observed with astrocytes (Fig. 6B). Control experiments were also performed to verify that changes in the fluorescent gradient were not due to simply either the absence of glucose or the presence of DETA-NO (Table 1). Perfusion of cells

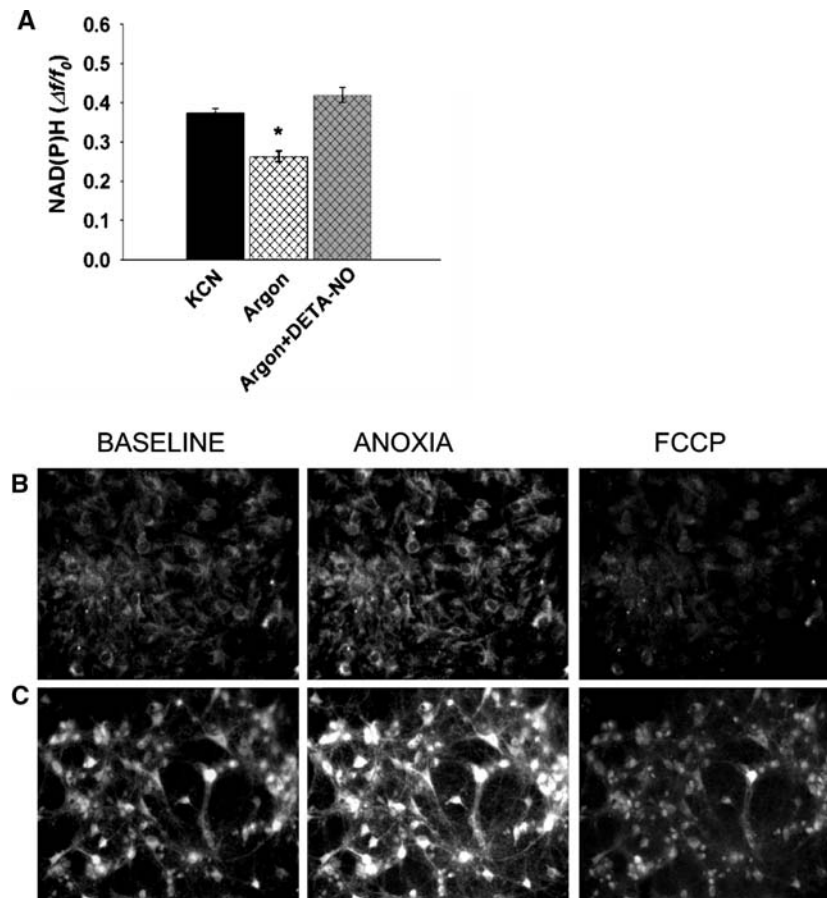


Fig. 3 Changes in NAD(P)H fluorescence induced by cyanide, argon, and a respiratory uncoupler. KCN-induced maximum increase in NAD(P)H autofluorescence in cortical neurons (control) was compared with the maximum increase in NAD(P)H autofluorescence when O_2 was displaced by continuous infusion of argon in the perfusate and the chamber (Argon) and DETA-NO $50 \mu\text{M}$ was added to the argon-bubbled perfusate (Argon+DETA-NO). Argon infusion in the absence of DETA-NO perfusion caused an increase in fluorescence that

was significantly lower than that observed in the presence of DETA-NO or with KCN ($n = 90\text{--}150$ cells measured during 3 separate experiments; $*p < 0.05$) (A). Examples of NAD(P)H autofluorescence images of cortical astrocytes (B) and cortical neurons (C) at selected time points: resting conditions (baseline), when maximum fluorescence was produced by anoxia and minimum fluorescence was produced by exposure to the respiratory uncoupler FCCP, $5 \mu\text{M}$

under either of these conditions in the absence of argon-induced O_2 depletion had no effect on the fluorescence increase caused by cyanide or the fluorescence decrease caused by FCCP with either neurons or astrocytes. We therefore conclude that it is the combination of hypoxia, DETA-NO and glucose deprivation that causes a diminution of the total pyridine nucleotide fluorescence gradient, specifically within cortical neurons.

Discussion

Intrinsic NAD(P)H fluorescence is a sensitive, non-invasive method for monitoring aerobic energy metabolism both in vitro and in vivo under normal and

pathological conditions. Both extreme levels of NAD(P)H reduction and oxidation have been proposed as indicators of mitochondrial dysfunction during reperfusion after brain ischemia [14–15]. Reperfusion-induced NAD(P)H hyperoxidation, neuronal dysfunction, and cell death are ameliorated by the presence of antioxidants [16] and by perfusion with normoxic compared to hyperoxic gas mixtures [17], suggesting that reactive oxygen species (ROS) mediate NAD(P)H hyperoxidation following anoxia.

In our experiments performed with essentially pure cultures of cortical neurons, we also observed a reoxygenation-induced, approximately 25% decrease in NAD(P)H fluorescence below the pre-anoxia baseline. The simplest explanation for this apparent oxidized shift in redox state is accelerated metabolism

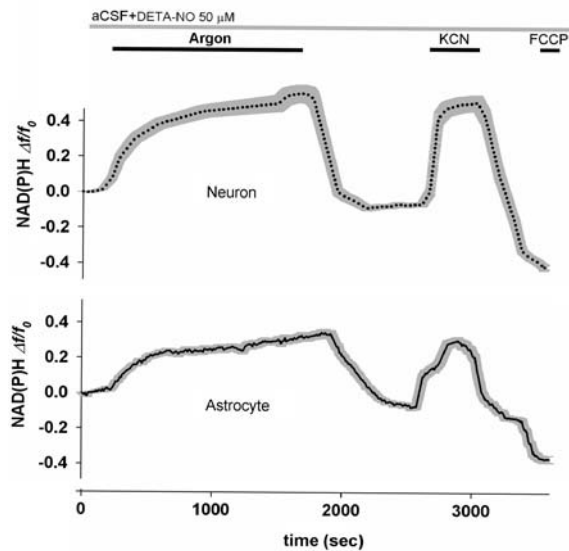


Fig. 4 Examples of changes in NAD(P)H fluorescence in cortical neurons (dotted line) and astrocytes (solid line) during anoxia induced by addition of DETA-NO 50 μ M in argon-bubbled perfusate containing glucose. Changes in NAD(P)H fluorescence reached a maximum by the time PO_2 levels reached their minimum (0–0.4 mm Hg) in both cell types and remained stable throughout the anoxic perfusion. KCN 1 mM and FCCP 5 μ M were added following reoxygenation to provide maximum and minimum NAD(P)H fluorescence, respectively. (Each trace represents the mean of fluorescence in cell somata in the field ($n = 30$ –50); gray shadow represents SEM)

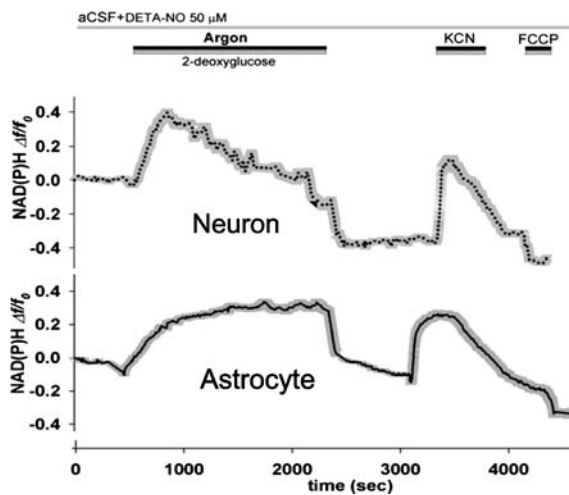


Fig. 5 Examples of changes in NAD(P)H fluorescence in cortical neurons (dotted line) and astrocytes (solid line) during anoxia induced by addition of DETA-NO 50 μ M in argon-bubbled perfusate containing 2-deoxyglucose and no glucose. Substitution of glucose by 2-deoxyglucose evoked a decline in the maximum NAD(P)H autofluorescence during anoxia and a significant rundown in fluorescence at reoxygenation in cortical neurons (dotted line) but not in astrocytes (solid line). Subsequent exposure to KCN did not restore the maximum NAD(P)H increase in cortical neurons

to compensate for the loss of ATP that occurs during metabolic anoxia. However, we also observed a gradual decline in autofluorescence during the 30 min period of anoxia and glucose deprivation, when oxidative energy metabolism is absent. This anoxia/reoxygenation-induced rundown in NAD(P)H autofluorescence was followed by a diminution in the fluorescence gradient between the value obtained upon addition of cyanide and that was obtained under normal conditions. Moreover, additional experiments demonstrated that the difference between the maximal fluorescence obtained with cyanide and the minimum obtained with the respiratory uncoupler FCCP was less following metabolic anoxia plus glucose deprivation than during control incubations or after metabolic anoxia plus glucose. This degradation of total pyridine nucleotide fluorescence suggests that a net loss of pyridine nucleotides occurs under these conditions. Alternatively, since pyridine nucleotide fluorescence is much greater when NADH is protein-bound rather than free, and since the majority of pyridine nucleotides are located within mitochondria [6,18–20], release of mitochondrial NADH into the cytosol could shift the equilibrium toward the unbound state, resulting in lower fluorescence.

While the nitric oxide-generating compound DETA-NO was included in our system along with argon to induce complete, metabolic anoxia, the nitric oxide so generated could also be indirectly responsible for loss of NAD(P)H fluorescence. For instance, nitric oxide and metabolites, e.g. peroxynitrite, can damage DNA, resulting in activation of the DNA repair enzyme, poly(ADP-ribose) polymerase-1 (PARP1), that consumes NAD^+ to form the non-fluorescent product, poly-(ADP ribose) [21]. While PARP1 activation can trigger cell death by several different pathways, depletion of NAD(H) and subsequent energy failure is one mechanism that has been demonstrated for neurons in response to hypoglycemia and hypoxia [22–24]. In addition, PARP1-mediated cortical neuronal death in response to neonatal hypoxia appears to be nitric oxide-dependent [25]. It is also possible that nitric oxide and other reactive nitrogen species activate the mitochondrial permeability transition [26], thereby lowering fluorescence through loss of mitochondrial matrix pyridine nucleotides. Nitric oxide could also promote the permeability transition indirectly via mitochondrial PARP1-mediated loss of NAD^+ [27].

In the presence of glucose, the pattern of changes in astrocyte NAD(P)H autofluorescence induced by metabolic anoxia followed by perfusion with normal medium, and then cyanide, was very similar to that of

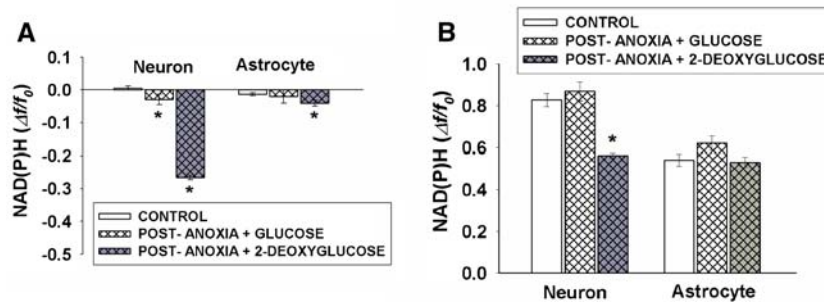


Fig. 6 Changes in NAD(P)H fluorescence relative to pre-anoxic baseline, at reintroduction of O₂ and glucose after 30 min of normoxic (control) or anoxic (± glucose and 2-deoxyglucose) perfusion (**A**). Fluorescence gradient between maximum fluorescence produced by KCN and minimum fluorescence produced

by respiratory uncoupler FCCP after normoxic perfusion (control) or anoxia/reoxygenation in cortical neurons and astrocytes. $n = 90\text{--}150$ cells measured during three separate experiments; * $p < 0.05$ compared to control

Table 1 Control experiments demonstrating no effect of glucose deprivation or DETA-NO on NAD(P)H fluorescent changes induced by cyanide and FCCP

		Neuron NAD(P)H (Δf/f)	Astrocyte NAD(P)H (Δf/f)
Control	Cyanide	0.493 ± 0.039	0.328 ± 0.031
	FCCP	-0.333 ± 0.025	-0.213 ± 0.025
+ DETA-NO	Cyanide	0.490 ± 0.036	0.296 ± 0.030
	FCCP	-0.295 ± 0.021	-0.221 ± 0.018
-Glucose	Cyanide	0.422 ± 0.020	0.359 ± 0.037
	FCCP	-0.325 ± 0.015	-0.228 ± 0.018

$n = 150\text{--}250$ cells measured during five separate experiments. DETA-NO, cyanide and FCCP were added as described in the experimental procedure

neurons. However, unlike neurons, in the absence of glucose, astrocyte pyridine nucleotide fluorescence was stable and no loss in the fluorescence with cyanide and after FCCP was observed. There was, however, a small but significant reduction in the fluorescent signal observed after reoxygenation following metabolic anoxia minus glucose compared to the baseline present prior to anoxia. The differences in responses of astrocytes and neurons to metabolic anoxia minus glucose and reoxygenation can be ascribed to the fact that astrocytes contain glycogen and neurons do not [28]. In addition to astrocytes possessing an endogenous source of glucose for anaerobic and post-anaerobic glycolysis, nitric oxide is known to stimulate glycolysis at the level of phosphofructokinase in astrocytes but not in neurons [29]. Maintenance of glycolysis by either exogenous or endogenous sources of glucose can protect against loss of NAD(P)H fluorescence by several mechanisms including the generation of reducing power necessary for reduction

of NAD⁺ and provision of ATP necessary for synthesis of NAD(H) depleted by PARP1 activity.

The different pyridine nucleotide fluorescence response of astrocytes and neurons during anoxia and reoxygenation may relate to the relative resistance of astrocytes to ischemia/reperfusion injury *in vivo*. For instance, if astrocyte glycolysis protects against NAD(H) degradation *in vivo*, they would be much less vulnerable than neurons to metabolic failure during reperfusion when both glycolysis and oxidative phosphorylation are needed and dependent on NAD⁺ for the activity of multiple dehydrogenases. Preservation of astrocyte metabolic integrity may also contribute to survival of neighboring neurons through astrocytic maintenance of active glutamate uptake [30] and trafficking of lactate as oxidative fuel for neurons [31].

In summary, we have developed an experimental system for continuous monitoring of NAD(P)H auto-fluorescence of cultured neurons and astrocytes during and after anoxia and glucose deprivation. While several measures were taken to lower the perfusate [O₂] to a level that would induce complete metabolic anoxia, the presence of a normally non-toxic level of nitric oxide was necessary to achieve the same level of pyridine nucleotide reduction as that seen in the presence of cyanide. Under these conditions, a partially irreversible loss of NAD(P)H fluorescence occurs in neurons but not astrocytes. This loss may be due to catabolism of NAD(H), e.g. by PARP1 activity, or by a shift in NADH from the protein bound to unbound state, e.g., what could occur following release of pyridine nucleotides from the mitochondrial matrix during the membrane permeability transition.

Acknowledgments These studies were supported by NIH grants NS34152, NS07375 and HD16596.

References

- Chance B, Williams GR (1955) Respiratory enzymes in oxidative phosphorylation. I Kinetics of oxygen utilization. *J Biol Chem* 217:383–393
- Chance B (2004) Mitochondrial NADH redox state, monitoring discovery and deployment in tissue. *Methods Enzymol* 385:361–370
- Williamson JR, Herczeg BE, Coles HS, Cheung WY (1967) Glycolytic control mechanisms. V. Kinetics of high energy phosphate intermediate changes during electrical discharge and recovery in the main organ of *Electrophorus electricus*. *J Biol Chem* 242:5119–5124
- Schuchmann S, Kovacs R, Kann O, Heinemann U, Buchheim K (2001) Monitoring NAD(P)H autofluorescence to assess mitochondrial metabolic functions in rat hippocampal-entorhinal cortex slices. *Brain Res Brain Res Protoc* 7:267–276
- Klaidman LK, Leung AC, Adams Jr. JD (1995) High-performance liquid chromatography analysis of oxidized and reduced pyridine dinucleotides in specific brain regions. *Anal Biochem* 228:312–317
- Vishwasrao HD, Heikal AA, Kasischke KA, Webb WW (2005) Conformational dependence of intracellular NADH on metabolic state revealed by associated fluorescence anisotropy. *J Biol Chem* 280:25119–25126
- Mayevsky A, Zarchin N, Kaplan H, Haveri J, Haselgroove J, Chance B (1983) Brain metabolic responses to ischemia in the mongolian gerbil: in vivo and freeze trapped redox scanning. *Brain Res* 276:95–107
- Perez-Pinzon MA, Mumford PL, Carranza V, Sick TJ (1998) Calcium influx from the extracellular space promotes NADH hyperoxidation and electrical dysfunction after anoxia in hippocampal slices. *J Cereb Blood Flow Metab* 18:215–221
- Tanaka K, Dora E, Greenberg JH, Reivich M (1986) Cerebral glucose metabolism during the recovery period after ischemia—its relationship to NADH-fluorescence, blood flow, EcoG and histology. *Stroke* 17:994–1004
- Welsh FA, Marcy VR, Sims RE (1991) NADH fluorescence and regional energy metabolites during focal ischemia and reperfusion of rat brain. *J Cereb Blood Flow Metab* 11:459–465
- Kasischke KA, Vishwasrao HD, Fisher PJ, Zipfel WR, Webb WW (2004) Neural activity triggers neuronal oxidative metabolism followed by astrocytic glycolysis. *Science* 305:99–103
- Brown GC, Cooper CE (1994) Nanomolar concentrations of nitric oxide reversibly inhibit synaptosomal respiration by competing with oxygen at cytochrome oxidase. *FEBS Lett* 356:295–298
- Cleeter MW, Cooper JM, Darley-Usmar VM, Moncada S, Schapira AH (1994) Reversible inhibition of cytochrome c oxidase, the terminal enzyme of the mitochondrial respiratory chain, by nitric oxide. Implications for neurodegenerative diseases. *FEBS Lett* 345:50–54
- Shiino A, Matsuda M, Handa J, Chance B (1998) Poor recovery of mitochondrial redox state in CA1 after transient forebrain ischemia in gerbils. *Stroke* 29:2421–2424
- Perez-Pinzon MA, Mumford PL, Carranza V, Sick TJ (1998) Calcium influx from the extracellular space promotes NADH hyperoxidation and electrical dysfunction after anoxia in hippocampal slices. *J Cereb Blood Flow Metab* 18:215–221
- Perez-Pinzon MA, Mumford PL, Rosenthal M, Sick TJ (1997) Antioxidants, mitochondrial hyperoxidation and electrical recovery after anoxia in hippocampal slices. *Brain Res* 754:163–170
- Feng ZC, Sick TJ, Rosenthal M (1998) Oxygen sensitivity of mitochondrial redox status and evoked potential recovery early during reperfusion in post-ischemic rat brain. *Resuscitation* 37:33–41
- Chance B, Baltscheffsky H (1958) Respiratory enzymes in oxidative phosphorylation. VII. Binding of intramitochondrial reduced pyridine nucleotide. *J Biol Chem* 233:736–739
- Shuttleworth CW, Brennan AM, Connor JA (2003) NAD(P)H fluorescence imaging of postsynaptic neuronal activation in murine hippocampal slices. *J Neurosci* 23:3196–3208
- Blinova K, Carroll S, Bose SA, Smirnov V, Harvey JJ, Knutson JR, Balaban RS (2005) Distribution of mitochondrial NADH fluorescence lifetimes: steady-state kinetics of matrix NADH interactions. *Biochemistry* 44:2585–2594
- Dawson VL, Dawson TM (2004) Deadly conversations: nuclear-mitochondrial cross-talk. *J Bioenerg Biomembr* 36:287–294
- Suh SW, Aoyama K, Chen Y, Garnier P, Matsumori Y, Gum E, Liu J, Swanson RA (2003) Hypoglycemic neuronal death and cognitive impairment are prevented by poly(ADP-ribose) polymerase inhibitors administered after hypoglycemia. *J Neurosci* 23:10681–10690
- Suh SW, Aoyama K, Matsumori Y, Liu J, Swanson RA (2005) Pyruvate administered after severe hypoglycemia reduces neuronal death and cognitive impairment. *Diabetes* 54:1452–1458
- Tanaka S, Takehashi M, Iida S, Kitajima T, Kamanaka Y, Stedeford T, Banasik M, Ueda K (2005) Mitochondrial impairment induced by poly(ADP-ribose) polymerase-1 activation in cortical neurons after oxygen and glucose deprivation. *J Neurochem* 95:179–190
- Mishra OP, Akhter W, Ashraf QM, Delivoria-Papadopoulos M (2003) Hypoxia-induced modification of poly (ADP-ribose) polymerase and dna polymerase beta activity in cerebral cortical nuclei of newborn piglets: role of nitric oxide. *Neuroscience* 119:1023–1032
- Bal-Price A, Brown GC (2000) Nitric-oxide-induced necrosis and apoptosis in PC12 cells mediated by mitochondria. *J Neurochem* 75:1455–1464
- Du L, Zhang X, Han YY, Burke NA, Kochanek PM, Watkins SC, Graham SH, Carcillo JA, Szabo C, Clark RS (2003) Intra-mitochondrial poly(ADP-ribosylation) contributes to NAD⁺ depletion and cell death induced by oxidative stress. *J Biol Chem* 278:18426–18433
- Ignacio PC, Baldwin BA, Vijayan VK, Tait RC, Gorin FA (1990) Brain isozyme of glycogen phosphorylase: immunohistological localization within the central nervous system. *Brain Res* 529: 42–9
- Almeida A, Moncada S, Bolanos JP (2004) Nitric oxide switches on glycolysis through the AMP protein kinase and 6-phosphofructo-2-kinase pathway. *Nat Cell Biol* 6:45–51
- Swanson RA (1992) Astrocyte glutamate uptake during chemical hypoxia in vitro. *Neurosci Lett* 147:143–146
- Magistretti PJ, Pellerin L, Rothman DL, Shulman RG (1999) Energy on demand. *Science* 283:496–147